doi:10.1246/cl.2011.1154

Published on the web September 28, 2011

Tuning the Nitrogen Content and Porosity of Nanostructured Carbon Nitride Using Aminoclay as a Reactive Template

B. V. V. S. Pavan Kumar, K. K. R. Datta, and Muthusamy Eswaramoorthy*
Nanomaterials and Catalysis Lab, Chemistry and Physics of Materials Unit, DST Unit on Nanoscience, Jawaharlal Nehru Centre for Advanced Scientific Research, Jakkur, Bangalore-560064, India

(Received June 23, 2011; CL-110524; E-mail: eswar@jncasr.ac.in)

The use of two-dimensional templates like clay, in the synthesis of graphitic carbon nitrides, make it feasible to form exfoliated layer like structures by polymerization of the precursors in the clay galleries. We have used clay linked with aminopropyl groups, aminoclay, to template the carbon nitride into mesolamellar structures. By virtue of its aminopropyl groups, aminoclay is further capable of reacting along with the intercalated precursors to enrich the carbon content of the resulting carbon nitrides.

Carbon nitrides are promising candidates to complement carbons in several applications. By virtue of their inherent mechanical,[1] optical, catalytic, semiconducting, and tribological properties including low density, surface roughness, wear resistance, chemical inertness, and biocompatibility,[2] these materials have found use as catalysts,[3,4] support materials in direct methanol fuel cells,[5] coatings on biomedical implants,[6] and metal ion sensors.[7] The versatility of the material in these myriad applications is dictated by the nitrogen content, material texture, surface area, and particle size.[8] This is especially true in catalysis where tuning the surface area and nitrogen content determines the accessibility and distribution of active sites and also the band gap in the case of photocatalysts. Nitrogen content, however, has been varied mostly through physical methods like ion-beam-assisted deposition,[9] thermal treatment,[10] and laser ablation[11] and a few chemical routes employing nitrogen-rich and carbon-rich precursors.[12–14] Surface area, on the other hand, has often been tuned by template-based synthesis using silica nanoparticles,[15] mesoporous silica,[16,17] and colloidal crystals[18] as three-dimensional templates. The use of two-dimensional templates would allow lateral polymerization of the precursors and restrict it in the z direction resulting in thin sheets which would be of interest in studying the unique properties of few-layer graphitic C_3N_4 (g-C_3N_4).[19] A reactive template capable of performing the function of one of the precursors would have an added functionality of controlling the nitrogen content by use of a single precursor.

Herein, we report a facile route toward tuning the morphology of carbon nitride to obtain mesolamellar structure using clay linked with aminopropyl groups (aminoclay) as a sacrificial and reactive template. This reactive template strategy also allows us to vary the nitrogen content of the carbon nitride compounds using a single precursor.

Aminoclay used in our study is a hybrid layered material of 2:1 trioctahedral magnesium phyllosilicate having covalently linked aminopropyl pendants occupying the interlayer regions (Figure S1, Supporting Information; SI[31]). Though montmorillonite and ammonium saponite have been used for making carbon nitride nanosheets, they failed to replicate the mesolamellar structure of clays due to the poor dispersibility of these clays in water.[20] Aminoclay on the other hand is highly dispersible in water due to the protonation of the pendant amine groups, giving it a positive charge which assists in exfoliation.[21] Further, it has an interesting property that once dispersed it can be restacked by addition of a poor solvent, ethanol, and in the process, trap molecules from the solution. This behavior was exploited to prepare porous layered carbon by entrapping glucose molecules within nanobundles of aminoclay.[22] Here, we have trapped cyanamide, a small negatively charged molecule, in the galleries of clay to form a clay–cyanamide nanocomposite (1:2 weight ratio). Cyanamide owing to its acidic nature[23] ($pK_a \approx 1.1$) easily interacts with the protonated amino groups of clay[24] ($pK_a \approx 10.6$) to aid intercalation. The intercalation in aminoclay is evident from the low-angle X-ray diffraction (XRD) patterns shown in Figures 1b and 1c. The low-angle peak associated with d_{001} spacing of aminoclay[21] at $2\theta = 5.4°$ (16.3 Å) shifted to 4.6° (19.1 Å) indicating an increase in d_{001} spacing due to the trapping of cyanamide in the interlayer space. The shift in d_{001} spacing of the clay is very minimal (2.8 Å) due to the small size of the cyanamide molecule. Its good solubility in water as well as ethanol prevents excess intercalation which is in contrast to the large amount of glucose trapping we have observed in the preparation of porous layered carbon due to the poor solubility of glucose in ethanol. The small size of the cyanamide molecules make it possible to infiltrate into the array of aminopropyl chains as depicted in Scheme 1. The infrared (IR) spectra of the nanocomposite show a peak at 2250 cm^{-1}(C≡N stretching) characteristic of cyanamide along with other peaks of clay[25] (Figure S2, SI[31]), which confirm that the cyanamide occupying the clay galleries retains

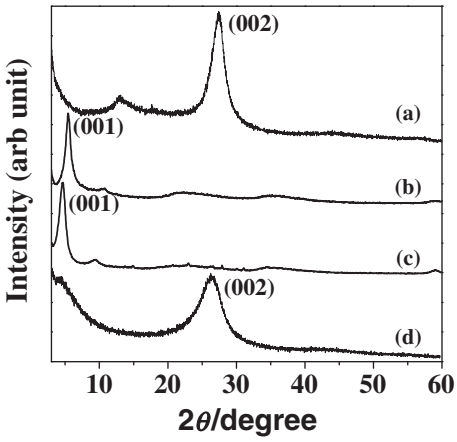

Figure 1. XRD patterns of (a) C_3N_4, (b) aminoclay, (c) clay–cyanamide nanocomposite and (d) mesolamellar C_3N_2.

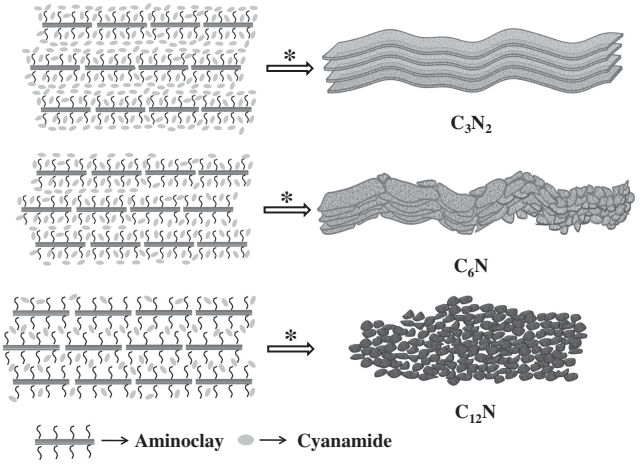

Scheme 1. Illustration showing the formation mechanism of morphology and composition of carbon nitride compounds (*calcination and demineralization).

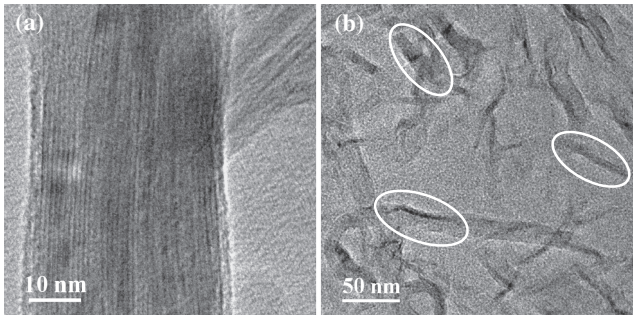

Figure 2. TEM images (a) showing the mesolamellar cross section and (b) exfoliated layers of C_3N_2 (circled in white).

its molecular identity. To obtain the mesolamellar carbon nitride, the cyanamide present in the clay galleries was allowed to polymerize by carbonizing the clay–cyanamide nanocomposite at 550 °C in nitrogen, followed by acid etching to remove inorganic remains of the clay. The observation of broad low-angle peak in the XRD pattern (Figure 1d) confirms that the mesolamellar structure is retained to a certain extent even after the removal of clay template. Transmission electron microscopy (TEM) image further supports the lamellar nature of the carbon nitride with the spacing between the layers about 0.6 nm which is roughly the thickness (of the inorganic part) of a single layer of aminoclay (Figure 2a). Cyanamide when polymerized at 550 °C gives a bulk material with a composition of g-C_3N_4 without any mesostructure. This suggests that polymerization of cyanamide in the confines of the mesolamellar structure of clay gives sub-nanometer thick sheets of carbon nitride which would otherwise give bulk carbon nitride with tightly bound graphitic layers. The TEM image also shows the existence of regions where exfoliated layers of carbon nitride structures dominate (Figure 2b). The chemical composition estimated from CHN analysis was found to be C_3N_2 (Figure 2b). The X-ray photoelectron spectroscopy (XPS) characterization was done to understand the nature of the bonding of nitrogen. The C1s and N1s spectra of the C_3N_2 sheets are given in the Figure S5 (SI[31]). The C1s spectra is deconvoluted into three peaks with binding energies at about 284.3, 285.2, and 288.0 eV representing pure graphitic sites, sp^2 carbon atoms bonded to nitrogen inside the aromatic ring, and sp^2 carbon atoms in the aromatic ring bonded to NH_2, respectively.[26] Similarly, the N1s spectrum is deconvoluted into three peaks with binding energies at 398.3, 400.1, and 401.6 eV which are attributed to the pyridinic nitrogen, pyrrolic nitrogen, and nitrogen incorporated into graphene layer, respectively.[27] This clearly shows that the nitrogen is an integral part of C_3N_2 sheets. This is further confirmed by elemental mapping which shows homogeneous distribution of carbon and nitrogen (Figure S6, SI[31]). The IR spectra of C_3N_2 shows a decrease in intensity of C–N (1350–1000 cm^{-1}), C=N (1680–1500 cm^{-1}), and N–H (1600–1500 cm^{-1}) stretching frequency with respect to the bulk C_3N_4 (Figure S3a, SI[31]). This, along with CHN data clearly suggests that the aminopropyl groups present in the clay condense with the cyanamide and, hence, enrich the carbon content of the resulting carbon nitride compounds. The Brunauer–Emmett–Teller (BET) surface area of C_3N_2, however, was found to be 21 $m^2 g^{-1}$, a marginal improvement over bulk C_3N_4 (14 $m^2 g^{-1}$). This implies that the entry to the pores would have probably been restricted by the fastening of adjoining layers due to strong interaction between carbon nitride sheets.

The extent of intercalation of cyanamide was studied by precipitating the clay from dispersion containing different weight ratios of clay and cyanamide. The degree of intercalation was monitored through low-angle XRD. The low-angle XRD patterns of the clay–cyanamide nanocomposites show gradual increase in interlayer spacing of clay with increase in cyanamide content in the precipitating medium, indicating an increase in the amount of cyanamide intercalation (Figure S4a, SI[31]). When the clay–cyanamide ratio was 2:1 in the composite, the d_{001} aminoclay peak shifted from 16.3 to 18.3 Å (about 2 Å drift) and for the ratio 5:1, the drift was nearly 1.4 Å (Figure S4a, SI[31]). The characteristic cyanamide peak observed in the IR spectrum at 2250 cm^{-1} (C≡N) shows that cyanamide occupying the clay galleries retains its molecular identity. On carbonization and demineralization with acids, the 2:1 and 5:1 clay–cyanamide nanocomposites gave compositions of C_6N and $C_{12}N$, respectively, showing a significant decrease in the nitrogen content due to the higher carbon contribution from the aminoclay. Depending on the relative amount of cyanamide trapped in the clay galleries the nitrogen content of the carbon nitride compounds is tuned accordingly. Less intercalation gives rise to carbon nitride with low nitrogen content. The thermogravimetric analyses show that the greater the nitrogen content, the greater the thermal stability of carbon nitrides (Figure S4b, SI[31]). However, it is to be noted that the decrease in particle size observed for C_6N and $C_{12}N$ (in comparison to C_3N_2 and C_3N_4) could also be the reason for their low thermal stability.

The TEM images of both C_6N and $C_{12}N$ are shown in Figure 3. $C_{12}N$ shows particulate-like structure, whereas C_6N shows lamellar structure in addition to particulate morphology. Correspondingly, the wide-angle XRD patterns of the C_6N and $C_{12}N$ showed increased broadening of the d_{002} peak (Figure 4a). As the nitrogen content in the carbon nitride decreases, the d_{002} spacing shows a gradual increase[13] (Figure 4a). The d_{002} for g-C_3N_4 is 3.27 Å, for graphite is 3.35 Å, and for turbostratically ordered graphite, it can go up to 3.7 Å.[28] Higher packing density with increasing nitrogen content is attributed to the localization of electrons and stronger binding between the layers.[29]

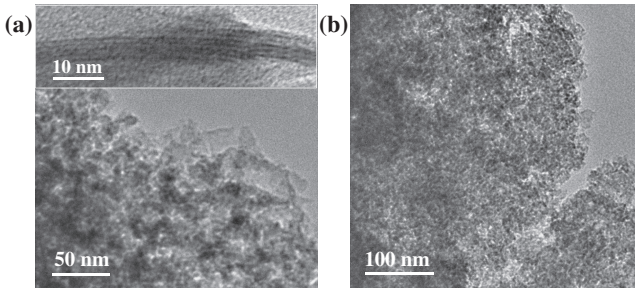

Figure 3. TEM images (a) showing both mesolamellar structure (top) and particulate nature of C_6N (bottom) and (b) showing porous particulate morphology of $C_{12}N$.

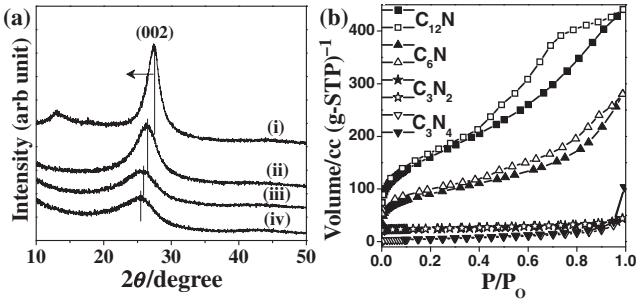

Figure 4. (a) Wide-angle XRD patterns of (i) C_3N_4, (ii) C_3N_2, (iii) C_6N, and (iv) $C_{12}N$. (b) N_2 adsorption (closed symbols)–desorption (open symbols) isotherms of carbon nitride compounds (C_3N_2 have been shifted by 20 units along the *y* axis).

Nitrogen adsorption–desorption isotherms of bulk C_3N_4, C_3N_2, C_6N, and $C_{12}N$ are shown in the Figure 4b. The nitrogen isotherms reveal a high level of porosity for both C_6N and $C_{12}N$ in contrast to the nonporous mesolamellar sheets of C_3N_2. The BET surface area for C_6N was calculated to be $330\,m^2\,g^{-1}$ and for $C_{12}N$ to be $580\,m^2\,g^{-1}$. The isotherm of C_6N shows a type-II b curve with a hysteresis loop of H3 type, indicative of the presence of slit-shaped pores or assemblages of platy particles typical of clay-templated materials.[30] The hysteresis in the isotherm of $C_{12}N$ is of H2 type, exhibited for interconnected pore networks. The observation of randomly fused particles in the TEM corroborates this hypothesis (Figure 3b).

Based on the experimental observations a common mechanism for the formation of carbon nitrides of different nitrogen content has been proposed in Scheme 1. When the clay–cyanamide nanocomposite is calcined at 550 °C the cyanamide molecules condense along with the aminopropyl groups which dilute the nitrogen content of the resulting carbon nitride. When the clay–cyanamide ratio is 1:2 the amount of cyanamide molecules intercalated in between the clay layers is sufficient to form the layered C_3N_2 structure on carbonization and demineralization. On the other hand, when the ratio is 5:1 (clay–cyanamide) the amount of cyanamide between the layers is very low to retain the layered structure on carbonization resulting in porous particulate morphology of composition, $C_{12}N$. In the case of 2:1 clay–cyanamide ratio, the extent of intercalation is not uniform, leading to domains of layered as well as particulate C_6N.

In order to increase the surface area of the mesolamellar C_3N_2, gold(III) chloride was reduced in situ to create Au nanoparticles in between the sheets to hold them apart and prevent to some extent the loss of surface area due to the collapse of the mesostructure by strong interlayer interaction (refer to Supporting Information).

In conclusion, we have used a water-dispersible two-dimensional template, aminoclay, to form mesolamellar structures of carbon nitride by polymerizing cyanamide in the clay galleries. Aminoclay acts as a reactive template and allows control over the nitrogen content with the use of a single precursor (cyanamide). Depending on the extent of intercalation in the aminoclay template the nitrogen content is tuned accordingly. The tunability of nitrogen content would find applications in modulating the conductivity, thermal stability, and catalytic properties of carbon nitride compounds.

BVVSPK thanks CSIR for research fellowship.

References and Notes

1 M. Kawaguchi, S. Yagi, H. Enomoto, *Carbon* **2004**, *42*, 345.
2 F. Z. Cui, D. J. Li, *Surf. Coat. Technol.* **2000**, *131*, 481, and references therein.
3 X. Wang, K. Maeda, A. Thomas, K. Takanabe, G. Xin, J. M. Carlsson, K. Domen, M. Antonietti, *Nat. Mater.* **2009**, *8*, 76.
4 Y. Ohgi, A. Ishihara, Y. Shibata, S. Mitsushima, K.-i. Ota, *Chem. Lett.* **2008**, *37*, 608.
5 M. Kim, S. Hwang, J.-S. Yu, *J. Mater. Chem.* **2007**, *17*, 1656.
6 D. J. Li, L. F. Niu, *Bull. Mater. Sci.* **2003**, *26*, 371.
7 E. Z. Lee, Y.-S. Jun, W. H. Hong, A. Thomas, M. M. Jin, *Angew. Chem., Int. Ed.* **2010**, *49*, 9706.
8 M. H. V. Huynh, M. A. Hiskey, J. G. Archuleta, E. L. Roemer, *Angew. Chem., Int. Ed.* **2005**, *44*, 737.
9 F. Alvarez, N. M. Victoria, P. Hammer, F. L. Freire, M. C. dos Santos, *Appl. Phys. Lett.* **1998**, *73*, 1065.
10 D. Hulicova, M. Kodama, H. Hatori, *Chem. Mater.* **2006**, *18*, 2318.
11 C. Niu, Y. Z. Lu, C. M. Lieber, *Science* **1993**, *261*, 334.
12 Y. Qiu, L. Gao, *Chem. Commun.* **2003**, 2378.
13 J. Zhang, X. Chen, K. Takanabe, K. Maeda, K. Domen, J. D. Epping, X. Fu, M. Antonietti, X. Wang, *Angew. Chem., Int. Ed.* **2010**, *49*, 441.
14 E. Frackowiak, G. Lota, J. Machnikowski, C. Vix-Guterl, F. Béguin, *Electrochim. Acta* **2006**, *51*, 2209.
15 F. Goettmann, A. Fischer, M. Antonietti, A. Thomas, *Angew. Chem., Int. Ed.* **2006**, *45*, 4467.
16 A. Vinu, K. Ariga, T. Mori, T. Nakanishi, S. Hishita, D. Golberg, Y. Bando, *Adv. Mater.* **2005**, *17*, 1648.
17 M. Kodama, J. Yamashita, Y. Soneda, H. Hatori, K. Kamegawa, I. Moriguchi, *Chem. Lett.* **2006**, *35*, 680.
18 S. Hwang, S. Lee, J.-S. Yu, *Appl. Surf. Sci.* **2007**, *253*, 5656.
19 M. Deifallah, P. F. McMillan, F. Corà, *J. Phys. Chem. C* **2008**, *112*, 5447.
20 G. Jiang, C.-H. Zhou, X. Xia, F. Yang, D. Tong, W. Yu, S. Liu, *Mater. Lett.* **2010**, *64*, 2718.
21 A. J. Patil, E. Muthusamy, S. Mann, *Angew. Chem., Int. Ed.* **2004**, *43*, 4928.
22 K. K. R. Datta, D. Jagadeesan, C. Kulkarni, A. Kamath, R. Datta, M. Eswaramoorthy, *Angew. Chem., Int. Ed.* **2011**, *50*, 3929.
23 S. Soloway, A. Lipschitz, *J. Org. Chem.* **1958**, *23*, 613.
24 P. Chaturbedy, D. Jagadeesan, M. Eswaramoorthy, *ACS Nano* **2010**, *4*, 5921.
25 S. L. Burkett, A. Press, S. Mann, *Chem. Mater.* **1997**, *9*, 1071.
26 A. Vinu, P. Srinivasu, D. P. Sawant, T. Mori, K. Ariga, J.-S. Chang, S.-H. Jhung, V. V. Balasubramanian, Y. K. Hwang, *Chem. Mater.* **2007**, *19*, 4367.
27 R. J. White, M. Antonietti, M.-M. Titirici, *J. Mater. Chem.* **2009**, *19*, 8645.
28 F. Tuinstra, J. L. Koenig, *J. Chem. Phys.* **1970**, *53*, 1126.
29 A. Thomas, A. Fischer, F. Goettmann, M. Antonietti, J.-O. Müller, R. Schlögl, J. M. Carlsson, *J. Mater. Chem.* **2008**, *18*, 4893.
30 F. Rouquerol, J. Rouquerol, K. Sing, *Adsorption by Powders and Porous Solids: Principles, Methodology and Applications*, Academic Press, Great Britain, **1999**.
31 Supporting Information is available electronically on the CSJ-Journal Web site, http://www.csj.jp/journals/chem-lett/index.html.

